Auto-regressive Discrete Acquisition Points Transformation for Diffusion Weighted MRI Data

Metcalfe-Smith, Emma; Meeus, Emma; Novak, Jan; Dehghani, Hamid; Peet, Andrew; Zarinabad, Niloufar

DOI:
10.1109/TBME.2019.2893523

Document Version
Publisher's PDF, also known as Version of record

Citation for published version (Harvard):
Metcalfe-Smith, E, Meeus, E, Novak, J, Dehghani, H, Peet, A & Zarinabad, N 2019, 'Auto-regressive Discrete Acquisition Points Transformation for Diffusion Weighted MRI Data', *IEEE Transactions on Biomedical Engineering*, vol. 66, no. 9, pp. 2617-2628. https://doi.org/10.1109/TBME.2019.2893523

Auto-regressive Discrete Acquisition Points Transformation for Diffusion Weighted MRI Data

Emma Metcalfe-Smith, *Student Member, IEEE*, Emma M. Meeus, Jan Novak, Hamid Dehghani, and Andrew C Peet*, Niloufar Zarinabad*

Abstract— ***Objective*: A new method for fitting Diffusion-Weighted Magnetic Resonance Imaging (DW-MRI) data composed of an unknown number of multi-exponential components is presented and evaluated. *Methods*: The Auto-regressive Discrete Acquisition Points Transformation (ADAPT) method is an adaption of the auto-regressive moving average system, which allows for the modelling of multi-exponential data and enables the estimation of the number of exponential components without prior assumptions. ADAPT was evaluated on simulated DW-MRI data. The optimum ADAPT fit was then applied to human brain DWI data and the correlation between the ADAPT coefficients and the parameters of the commonly used bi-exponential Intravoxel Incoherent Motion (IVIM) method were investigated. *Results*: The ADAPT method can correctly identify the number of components and model the exponential data. The ADAPT coefficients were found to have strong correlations with the IVIM parameters. ADAPT(1,1)-β_0 correlated with IVIM-D: ρ=0.708, P <0.001. ADAPT(1,1)-α_1 correlated with IVIM-f: ρ=0.667, P <0.001. ADAPT(1,1)-β_1 correlated with *IVIM-D*:* ρ=0.741, P <0.001). *Conclusion*: ADAPT provides a method that can identify the number of exponential components in DWI data without prior assumptions, and determine potential complex diffusion biomarkers. *Significance*: ADAPT has the potential to provide a generalized fitting method for discrete multi-exponential data, and determine meaningful coefficients without prior information.**

***Index Terms*— Multi-exponential fitting, Diffusion MRI, Robustness**

Manuscript received May 18, 2018, revised October 19 2018, accepted January 8 2019. This work was funded by the Engineering and Physical Sciences Research Council (EPSRC) through a studentship from the Sci-Phy-4-Health Centre for Doctoral Training (EP/L016346/1) and the Physical Sciences of Imaging in Biomedical Sciences (PSIBS), Doctoral Training Centre (EP/F50053X/1), the National Institute for Health Research (NIHR) via a research professorship (13-0053), the Paediatric Experimental Cancer Medicine Centre and Free Radio in conjunction with Help Harry Help Others (HHHO). Asterisk indicates joint senior and corresponding authors.

E. Metcalfe-Smith is with the Physical Sciences for Health, Doctoral Training Centre, University of Birmingham and the Institute of Cancer and Genomic Sciences, University of Birmingham. They are also with the Department of Oncology, Birmingham Children's Hospital.

EM Meeus was with the Physical Sciences of Imaging in Biomedical Sciences, Doctoral Training Centre, University of Birmingham and the Institute of Cancer and Genomic Sciences, University of Birmingham. They were also with the Department of Oncology, Birmingham Children's Hospital. She is now an honorary member of the Institute of Cancer and Genomic Sciences, University of Birmingham and the Department of Oncology, Birmingham Children's Hospital.

J Novak was with the Institute of Cancer and Genomic Sciences, University of Birmingham and the Department of Oncology, Birmingham Children's Hospital. He is now an honorary member of the Institute of Cancer and Genomic Sciences, University of Birmingham and the Department of Oncology, Birmingham Children's Hospital.

H Dehghani is with the School of Computer Science, University of Birmingham. They are also with the Physical Sciences for Health, Doctoral Training Centre, University of Birmingham.

AC Peet is with the Institute of Cancer and Genomic Sciences, University of Birmingham and the Department of Oncology, Birmingham Children's Hospital. (email: a.peet@bham.ac.uk)

N Zarinabad was with the Institute of Cancer and Genomic Sciences, University of Birmingham, Birmingham, B15 2TT, UK and the Department of Oncology, Birmingham Children's Hospital, Birmingham, B4 6NH. She is now an honorary member of the Institute of Cancer and Genomic Sciences, University of Birmingham and the Department of Oncology, Birmingham Children's Hospital.(email: N.Zarin@bham.ac.uk)

I. Introduction

MULTI-EXPONENTIAL fitting is a challenging task for diffusion-weighted magnetic resonance imaging (DW-MRI) data, where there are a limited number of data points and the number of components within the diffusion signal is unknown. Both theoretical and experimental studies have suggested that the water diffusion in tissue is characterized by multi-exponential behavior [1], [2], [3]. Diffusion weighted imaging (DWI) has been demonstrated to have clinical relevance for identifying areas of cerebral ischemia and oncological diagnosis [4]. As the reported diffusion coefficient is dependent upon the fitting method implemented, it is crucial that the optimum method is realized.

In order to attain the diffusion coefficient for each voxel in the MR image, the scan is repeated at different b-values [5], a parameter that is changed by varying the diffusion sensitization of the MR sequence. If a gradient pulse is applied during the MR scan, a phase shift in the proton precession is induced. If an exact reverse gradient is subsequently applied, particles that have moved, via diffusion, will experience at net phase shift and the detected signal intensity will attenuate. The b-value is related to the duration, strength and time-spacing of these two gradient pulses. As the b-values increase, so does the sensitivity to particle motion, and the detected signal attenuates exponentially. By plotting the signal on a logarithmic scale and calculating the gradient, the diffusion coefficient for that voxel is attained [6]. The greater the signal attenuation, the greater the rate of diffusion.

$$S=\begin{bmatrix} b_{(0)} & 0 & \cdots & 0 & 0 & 0 & \cdots & 0 \\ b_{(1)} & b_{(0)} & \cdots & \vdots & ln\left(\frac{S_{(0)}}{S_{(0)}}\right) & 0 & \cdots & \vdots \\ \vdots & \vdots & \cdots & \vdots & ln\left(\frac{S_{(1)}}{S_{(0)}}\right) & ln\left(\frac{S_{(0)}}{S_{(0)}}\right) & \cdots & \vdots \\ \vdots & \vdots & \cdots & \vdots & \vdots & \vdots & \cdots & \vdots \\ b_{(N)} & b_{(N-1)} & \cdots & b_{(N-Q)} & ln\left(\frac{S_{(N-1)}}{S_{(0)}}\right) & ln\left(\frac{S_{(N-2)}}{S_{(0)}}\right) & \cdots & ln\left(\frac{S_{(N-P)}}{S_{(0)}}\right) \end{bmatrix}; A=\begin{bmatrix} \beta_0 \\ \vdots \\ \beta_Q \\ -\alpha_1 \\ \vdots \\ -\alpha_P \end{bmatrix}; S_{pred}=\begin{bmatrix} ln\left(\frac{S_{(0)}}{S_{(0)}}\right) \\ ln\left(\frac{S_{(1)}}{S_{(0)}}\right) \\ \vdots \\ ln\left(\frac{S_{(N)}}{S_{(0)}}\right) \end{bmatrix} \quad (2)$$

Multi-component models have been applied to DWI data previously, and the most common is the Intravoxel Incoherent Motion (IVIM) method [7]. The IVIM method assumes that the signal is composed of two exponentials, accounting for tissue water diffusion and bulk flow in small blood vessels. When plotted on a logarithmic scale, the gradient of each component provides the diffusion related coefficients for each exponential term. If IVIM is fitted using the Levenberg-Marquardt algorithm, initial starting values for the parameters are required, and the fitting stability is often improved by using a multistep fitting approach [8]. However, additional physical processes such as multiple diffusion rates within one physical component, bulk flow in tubules or glandular secretion may also affect the detected signal, which leads to more than two exponential components [9]. Hence, a method with the ability to optimize the number of components could provide a new insight into the physical properties of water motion in tissue.

Fitting of multi-exponential equations to experimental data is a notable problem for many different scientific fields. The number of exponential terms within a signal, the decay coefficients of each term along with the fractional value of each term, indicating each component's contribution to the overall signal, all have to be determined [10]. The accuracy of such models is of particular importance in the biomedical field, where multi-exponential decay is common and robust biomarkers are required. The complex fitting problem is therefore further exacerbated by the poor signal to noise ratios (SNRs) and a limited number of data points [11].

Common exponential fitting methods such as graphical methods are simple to execute, but are subjective and prone to high errors [12]. Parametric techniques, which provide a solution as a series of damped sinusoids [13], are also commonly implemented, but are restricted to data equally spaced in time [11]. These algorithms have also been demonstrated to be highly susceptible to noise and perform poorly when trying to determine the number of exponential terms in signals with a large number of components [10], [11]. Transform methods have also been developed [10], in which the data is Fourier transformed to create a spectral plot with spikes representing exponential components [11]. However, this approach exacerbates high frequency noise in the deconvolution process [14], causing ripples and broadening of the spectral peaks, making interpretations of the results difficult. Overall, there is a need to develop improved analysis methods for multi-exponential data.

Auto Regressive Moving Average (ARMA) models [15] are generalized versions of multi-exponential models and can predict the behavior of a data series from previous values alone. ARMA has the flexibility to represent a wide range of data series, with the order (number of lag terms) of the optimum ARMA model relating to the complexity of the data. However, such a method is restricted to the time domain. To adapt the method for the modeling of DWI data, the ARMA model was modified, henceforth referred to as the Auto-regressive Discrete Acquisition Points Transformation (ADAPT) method. ADAPT interprets the discrete signal as a function of acquisition points. Although there is no simple relationship between the IVIM parameters and ADAPT coefficients, ADAPT presents the opportunity for novel diffusion biomarkers to be obtained with no prior assumption about the nature of the data. Futhermore, ADAPT does not require any multistep fitting processes, unlike other DWI fitting methods. The aim of this study was therefore to develop a new generalized fitting method for multi-exponential data where the number of components is unknown a priori and evaluate it on simulated and real multi b-value DWI data

II. Materials and Methods

A. The Auto-regressive Discrete Acquisition Points Transformation (ADAPT) Method

ADAPT models the diffusion signal by the equation:

$$\ln(S_n)=\sum_{i=0}^{Q}\beta_i b_{n-i}+\sum_{j=1}^{P}\alpha_j \ln(S_{n-j}) \quad (1)$$

Where S_n-Signal at acquisition point n; b_n- b-value at acquisition time point n. α_j, β_i- minimisation coefficients. Here the acquisition point of the b-values is used such that b value=0 s/mm^2 at acquisition point 0, b(0)=0. b-value=20 s/mm^2 at acquisition point 1, b(1)=20 and so forth. The previously acquired b-values are therefore used as previous input terms. Upon selecting the order of the ADAPT(P,Q) model, the α and β minimization coefficients are determined such that the error between the data and the model is minimized. The coefficients are determined via establishing the matrices in (2), stated above. S is a matrix engineered from the input b-values and the detected signal with acquisition point n=0, …, N. A is the matrix of ADAPT coefficients. S_{pred} is the final model of the predicted signal normalised by S(0)- the initial signal value at b=0 and n=0. By finding the least

squares error of (3), the ADAPT coefficients are minimised and the model S_{pred} is established:

$$S \cdot A = S_{pred} \quad (3)$$

1) Determining the Number of Components

Upon selection of the optimum ADAPT order, the transfer function can be expressed as (4):

$$H(n) = \frac{\ln(S_n)}{b_n} = \frac{\beta_0 + \beta_1 \hat{L} + \cdots + \beta_P \hat{L}^P}{1 - \alpha_1 \hat{L} - \cdots - \alpha_Q \hat{L}^Q} \quad (4)$$

Where $\hat{L}$ is the lag operator [16] such that $\ln(S_n)\,\hat{L} = \ln(S_{n-1})$. By mapping the transfer function of the optimum order to the Z-domain the following is obtained (5):

$$H(z) = \frac{\beta_0 + \beta_1 z^{-1} + \cdots + \beta_P z^{-P}}{1 - \alpha_1 z^{-1} - \cdots - \alpha_Q z^{-Q}} \quad (5)$$

Equation 5 can be rearranged using partial fraction decomposition. An inverse Z-transform was then performed and the number of components established. For example ADAPT(1,1) gives:

$$\ln(S_n) = \beta_0 b_n + \beta_1 b_{n-1} + \alpha_1 \ln(S_{n-1}) \quad (6)$$

Taking the transfer function of ADAPT(1,1) in the Z-domain and performing partial fraction decomposition (PFD) and an Inverse Z transform:

$$H(n) = \beta_1 {\alpha_1}^{n-1} + \beta_0 {\alpha_1}^{n} \quad (7)$$

Here ADAPT(1,1) is evaluated to be a two component decay model.

B. Data Simulations

All simulated and acquired in vivo data was created or obtained using a range of 11 exponentially spaced b-values between 0 and 1000 [0, 20, 40, 80, 110, 140, 170, 200, 300, 500, 1000] s/mm^2. All simulations and data analysis were conducted using MATLAB (MathWorks, Natick, MA, USA, v.2016b).

1) Simulation of a Bi-exponential Signal

A range of bi-exponential diffusion signals were created by simulating data using the equation for the IVIM method (8):

$$\frac{S(b)}{S(0)} = f \cdot \exp^{-bD^*} + (1 - f) \cdot \exp^{-bD} \quad (8)$$

Where S(b)/S(0) is the signal intensity for a particular b-value, b, normalized by the signal intensity when b=0 s/mm^2; D is the tissue diffusion coefficient; D* is the pseudo-diffusion coefficient (related to the perfusion of blood in the capillary network); and f is the volume fraction of incoherently flowing blood in the tissue describing the fraction of the signal arising from the vascular network [6].

Bi-exponential signals were created with a range of f values (0.1, 0.3 and 0.5) and three different D*/D ratios corresponding to those observed in the brain, kidney and liver (10, 20 and 70 respectively) [17]. The D parameter was fixed at 0.0007 mm^2/s and the D* parameters considered were 0.007 mm^2/s, 0.014 mm^2/s and 0.049 mm^2/s. Random white Gaussian noise was added to the simulated signals to mimic SNR levels of 50, typical of those measured in in vivo data. The ADAPT method was applied to the bi-exponential signals, and a range of orders from ADAPT(0,0) to ADAPT(3,3) were considered.

2) Simulation of a Multi-Component Partial Volume Effects Model

A partial volume effects (PVE) model was simulated, in which compartments from both cerebral white matter (WM), assumed to be a two compartment model, and cerebrospinal fluid (CSF), assumed to be one compartment, are simultaneously detected, thus creating a tri-exponential model (9).

$$\frac{S(b)}{S(0)} = Ae^{-b\alpha} + Be^{-b\beta} + Ce^{-b\gamma} \quad (9)$$

Such a tissue model is of particular interest to DWI, as the use of the IVIM method in the brain requires cautious interpretation in regions of tissue edges due to PVE. The high value of the diffusion coefficient in CSF and the much lower diffusion coefficient in WM results in the incorrect detection of a large perfusion value within the cerebral cortex, when a voxel contains information from both these regions [18]. CSF was assumed to exhibit mono-exponential behavior with a diffusion coefficient assumed to be that of free water at 37℃ ($D_{CSF} = 3 \times 10^{-3}\text{mm}^2/\text{s}$) [19]. WM was assumed to be represented by the bi-exponential IVIM method. The WM model parameters were taken from averaged IVIM values previously reported in a volunteer study ($f_{WM} = 0.07; D_{WM} = 0.77 \times 10^{-3}\text{mm}^2/\text{s}; D^*_{WM} = 7.9 \times 10^{-3}\text{mm}^2/\text{s}$) [20]. A partial volume effect (PVE) model was created as a summation of the CSF and WM model such that (9) was parametrized with physically meaningful coefficients:

$$\frac{S(b)}{S(0)} = f_{CSF}e^{-bD_{CSF}} + (1 - f_{CSF})(f_{WM}e^{-bD^*_{WM}} + (1 - f_{WM})e^{-bD_{WM}}) \quad (10)$$

Where f_{CSF} indicated the fraction of the signal that was contributed by the CSF compartment. A range of PVE models were created with varying CSF:WM ratios (100:0, 75:25, 50:50, 25:75 and 0:100). White Gaussian noise was added to PVE models to mimic SNR levels ≈ 50.

3) Robustness Analysis

Poor signal quality can result in a change of parameter values or in the detection of an additional component. Hence the effects of poor SNR on the robustness of the fitting methods were investigated. Random white Gaussian noise was added to the simulated signals to mimic SNR levels between 20 and 100. Although the noise present in MRI data is governed by a Rician noise distribution, the distribution is nearly Gaussian for the SNR levels considered in this study [21]. Noise was added using the MATLAB Communications System Toolbox 'Add White Gaussian Noise' (awgn) function. The data simulations were performed using 1000 random data iterations for each model and SNR level.

C. In Vivo Data Acquisition

A volunteer brain scan (age 25 years), SNR≈50 in WM at b-value = 0 s/mm^2, was acquired on a Philips Achieva 3T TX (Philips Healthcare, Best, the Netherlands) MRI scanner at Birmingham Children's Hospital using a 32-multichannel receiver head coil. A brain tumour, suprasellar pilomyxoid astrocytoma, patient (age 3.2 years) was also scanned. The patient case was considered due to the ventricles being enlarged, allowing for an easier investigation of the one compartment CSF. It should be noted that no tumour was present on the slice considered. Informed parental consent was obtained for all subjects and the East Midlands – Derby Research Ethics Committee (REC 04/MRE04/41) approved the study operating under the rules of Declaration of Helsinki 1975 (and as revised in 1983). The diffusion-weighted MRI sequence used a sensitivity-encoded (SENSE) approach with the following parameters: b-value data acquired in three orthogonal directions, FOV 230mm x 230mm, TR/TE 3,214/84ms, matrix size 256x256, 5mm slice thickness and in plane resolution 0.9mm x 0.9mm. The spectral presaturation with inversion recovery (SPIR) was used for fat suppression and the scan duration was 2.21 minutes.

D. Data Analysis

1) Measuring SNR

In vivo SNR levels were calculated using the standard NEMA method based on the difference image from two acquisitions, this is the recommended method for determining SNR when parallel imaging techniques are used [22]. The quality of parameter estimation depends strongly on the SNR, with the SNR for the low IVIM perfusion regime recommended to be above a critical value of 40 [17][21]. A SNR≈50 was recorded in the White Matter (b-value =0), in agreement with previous studies using this acquisition protocol [8].

2) Model Selection

The Akaike information criterion (AIC) [23] was used as a means of model selection for determining the optimum ADAPT order. The AIC estimates the relative quality of each of the multiparametric fitting methods, rewarding for goodness of fit and penalizing for the complexity. Such a selection process aims to reduce the risk of over-fitting. As the b-value sequence used within the diffusion-weighted imaging (DWI) protocol typically has less than 30 b-values (11 in the cases considered), they can be considered to be a finite data set [3]. Thus the corrected AIC (AICc) [24], with a harsher penalty for over fitting, was implemented. The AICc formula (11):

$$\mathrm{AIC_c} = \mathrm{n} \cdot \log\left(\frac{\mathrm{RSS}}{\mathrm{n}}\right) + \frac{2 \cdot \mathrm{k} \cdot (\mathrm{k}+1)}{\mathrm{n}-\mathrm{k}-1} \tag{11}$$

Where n is the number of b-values used to fit the signal; k is the number of parameters; and RSS is the residual sum squared. The fit with the lowest AICc value is considered to be the optimum fit. The number of parameters, k, includes the diffusion signal S_0 [25] and an additional parameter is counted due to the Gaussian noise hypothesis for the signal residuals [3]. There is debate in the literature that the AIC is only suitable for analysing nested models and is consequently inherently biased. The authors believe that although the models in this study are nested, the AIC is a suitable criterion for a wide range of model types, both nested and non-nested [26]. To ensure that such a selection criterion is not ad-hoc, an additional selection criterion is also considered- the Bayesian Information Criterion corrected for small samples (BICc) [27].

It is advocated that an approach of using two criteria together can increase the confidence in identifying the optimum order [28], hence the BICc (12): was also calculated

$$\mathrm{BICc} = \frac{\mathrm{k} \cdot \mathrm{n} \cdot \log(\mathrm{n})}{n-k-1} + \mathrm{n} \cdot \log\left(\frac{\mathrm{RSS}}{\mathrm{n}}\right) \tag{12}$$

The relative significance of the optimum information criterion fit was justified with the used of Bayes Factors [29] (Appendix A). w_i is the Weight, indicating the probability of model i being the optimum model and the associated statistic the log evidence ratio (LER) indicates evidence for the parsimoniousness of the optimum model against a competing model. LER values greater than 0, 0.5, 1 or 2 indicate respectively that the evidence is 'minimal', 'substantial', 'strong' or 'decisive'.

3) Statistical Analysis

For the data simulations, correlation analysis (Pearson correlation coefficient, r) was performed to determine how the ADAPT(1,1) coefficient were related to the IVIM parameters. ADAPT(1,1) was considered as it was found to be the optimum fit for bi-exponential equations. The IVIM parameters were calculated using the multi-exponential fitting methods as described in the section below (II.D.3).The statistical significance of the relationship was assessed using the p-value (P <0.05). The robustness of the ADAPT and multi-exponential coefficients, when fitted to the PVE models, was assessed by calculating the coefficient of variation (CV) over the 1000 iterations measured.

For the in vivo data, correlation analysis (Spearman's rank correlation coefficient, ρ) was performed to compare the ADAPT(1,1) coefficients to the IVIM parameters. ρ values between 0.60-0.79, and 0.80-1.0, were considered to represent a 'strong' and 'very strong' correlation respectively. Five regions of interest (ROIs), each 4x4 pixels, were selected from within both the one compartment CSF and the two compartment WM. The ROIs were drawn upon the DWI scans with no additional filtering. The optimum ADAPT and multi-exponential fitting methods were fitted to each of the ROIs. To investigate the robustness of the fitting parameters, the average parameter value and CV was calculated.

4) Multi-exponential Fitting Methods

The bi-exponential fitting method for the IVIM equation was assessed using non-linear least squares minimization, with the Levenberg-Marquardt algorithm and a constrained 2-parameter fitting method [21]. The tri-exponential fitting method used the same minimization technique and a constrained 4-parameter fitting method. The mono-exponential fitting method was also considered for the PVE models and in vivo data. By plotting the signal on a logarithmic scale and calculating the gradient, the Apparent Diffusion Coefficient (ADC) is attained.

This article has been accepted for publication in a future issue of this journal, but has not been fully edited. Content may change prior to final publication. Citation information: DOI 10.1109/TBME.2019.2893523, IEEE Transactions on Biomedical Engineering

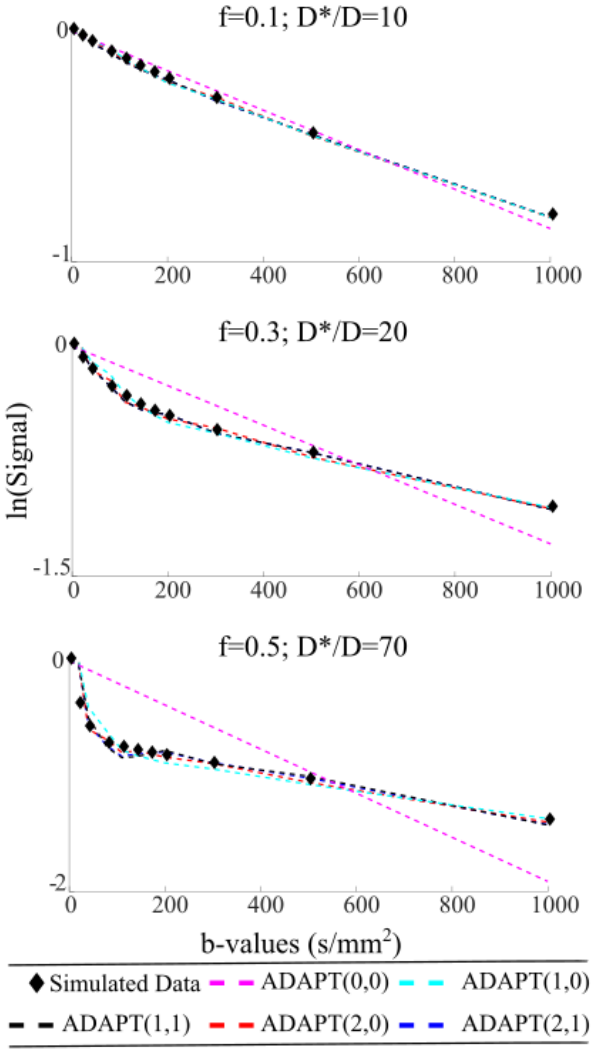

Fig.1. The ADAPT orders fitted to a range of simulated bi-exponential signals.

5) Performance of Fitting Methods

All calculations were performed on OS: Windows 10 Pro 64-bit (10.0 Build 16299), CPU: AMD Ryzen 5 1600, 3.2 GHz, Memory: 8192 MB DDR4 RAM. To compare the performance of the ADAPT and IVIM fitting methods, the CPU run time of each method was recorded and averaged over 10 iterations.

III. Results

A. ADAPT Method Applied to Simulated Bi-exponential Signal

1) Selection of Optimum Fit

A range of ADAPT orders were fitted to the simulated bi-exponential signal (SNR ≈ 50) with varying IVIM parameters (Fig.1). For each of the 9 scenarios considered ADAPT(1,1) was found to be the optimum order, having the lowest AICc for every case (Table I). For the bi-exponential signals where D*/D=10, the competing order ADAPT(2,1) was found to have an AICc-LER just below 0.5 in two instances. For the bi-exponential signals with D*/D=70 and f=0.3 or 0.5, the AICc-LER ratio indicates that ADAPT(1,0) and ADAPT(2,0) are

TABLE I
ADAPT Orders Fitted to Bi-exponential Diffusion Signals-AICc

			ADAPT Orders				
D*/D	**f**		**(0,0)**	**(1,0)**	**(1,1)**	**(2,0)**	**(2,1)**
10	0.1	AICc	-73	-97	**-120**	-97	-115
		LER_{AIC_c}	10.06	4.85	**0**	4.94	0.92
	0.3	AICc	-49	-79	**-101**	-80	**-98**
		LER_{AIC_c}	11.22	4.74	**0**	4.39	**0.49**
	0.5	AICc	-36	-68	**-91**	-69	**-89**
		LER_{AIC_c}	11.87	5.03	**0**	4.75	**0.42**
20	0.1	AICc	-65	-88	**-106**	-93	-103
		LER_{AIC_c}	8.93	3.88	**0**	2.98	0.67
	0.3	AICc	-39	-68	**-82**	-73	-79
		LER_{AIC_c}	9.35	3.12	**0**	2.02	0.70
	0.5	AICc	-25	-56	**-71**	-61	-68
		LER_{AIC_c}	9.90	3.21	**0**	2.07	0.70
70	0.1	AICc	-59	-78	**-84**	-80	-80
		LER_{AIC_c}	5.39	1.24	**0**	0.75	0.70
	0.3	AICc	-32	**-56**	**-58**	**-57**	-55
		LER_{AIC_c}	5.58	**0.48**	**0**	**0.23**	0.66
	0.5	AICc	-18	**-43**	**-45**	**-44**	-42
		LER_{AIC_c}	5.84	**0.39**	**0**	**0.09**	0.62

A range of two compartment bi-exponential diffusion signals (SNR≈50) were investigated with a range of IVIM-D*/D ratios and IVIM-f values. The ADAPT method was applied to the bi-exponential signals and the optimum fit (highlighted) was selected by choosing the method with the lowest AICc. Those ADAPT orders lightly shaded have an AICc-LER<0.5 indicating competing models.

competing orders that should also be taken into consideration. ADAPT orders (2,2), (3,0), (3,1), (3,2) and (3,3) were also considered for each case but possessed comparatively higher AICc values and thus very high AICc-LERs. The BICc confirmed that the optimum order was ADAPT(1,1) (Table II). No competing orders were detected when D*/D=10. For the signals with D*/D=70 and f=0.3 or 0.5, the BICc indicated that ADAPT(1,0) was the optimum order. However, the BICc-LER for ADAPT(1,1) was low and the BICc values almost equivalent.

2) Number of Components

The Transfer function, Z-transform, PFD and subsequent inverse Z-transform were performed on ADAPT(0,0), ADAPT(1,0), ADAPT(1,1), ADAPT(2,0) and ADAPT(2,1). ADAPT(0,0) is equivalent to the mono-exponential model and thus a one component decay model. As previously stated, ADAPT(1,1) was evaluated to be a two component decay model. In all bi-exponential simulations considered, a two component model was found to be the optimum fit, based upon the AICc. ADAPT(2,0) and ADAPT(2,1), which were found to be competing orders are also two-component decays models (Appendix B). ADAPT(1,0), a one component decay model (Appendix B), was found to be a competing order for some cases. However, for the D*/D ratio of 70 and f value of 0.3, the AICc-LER of ADAPT(1,0) is 0.48 is close to the cut off and the wi probability (ADAPT(1,0) wi=0.14) is more than half that of the optimum order (ADAPT(1,1) wi=0.43).). The BICc selected ADAPT(1,0) as the optimum order (wi=0.44), however, the BICc-LER for ADAPT(1,1) was very low, 0.12 and wi= 0.33. For the D*/D ratio of 70 and f-value of 0.5, the

TABLE II
ADAPT ORDERS FITTED TO BI-EXPONENTIAL DIFFUSION SIGNALS-BICC

			ADAPT Orders				
D*/D	**f**		**(0,0)**	**(1,0)**	**(1,1)**	**(2,0)**	**(2,1)**
10	0.1	BICc	-68	-89	**-109**	-86	-101
		LER_{BIC_c}	8.79	4.19	**0**	4.94	1.67
	0.3	BICc	-46	-74	**-93**	-72	-87
		LER_{BIC_c}	10.04	4.13	**0**	4.39	1.15
	0.5	BICc	-34	-63	**-83**	-61	-78
		LER_{BIC_c}	10.70	4.42	**0**	4.75	1.08
20	0.1	BICc	-63	-83	**-99**	-85	-92
		LER_{BIC_c}	7.76	3.28	**0**	2.98	1.33
	0.3	BICc	-37	-63	**-74**	-65	-68
		LER_{BIC_c}	8.18	2.51	**0**	2.02	1.36
	0.5	BICc	-23	-51	**-63**	-53	-57
		LER_{BIC_c}	8.72	2.61	**0**	2.07	1.36
70	0.1	BICc	-56	-73	**-76**	-72	-69
		LER_{BIC_c}	5.39	1.24	**0**	0.75	0.70
	0.3	BICc	-30	**-50**	**-50**	**-49**	-44
		LER_{BIC_c}	4.53	**0**	**0.12**	**0.35**	1.44
	0.5	BICc	-15	**-38**	**-37**	**-36**	-42
		LER_{BIC_c}	4.88	**0**	**0.21**	**0.30**	0.62

The optimum ADAPT order for the simulated bi-exponential diffusion signals was selected using the lowest BICc. Those ADAPT orders lightly shaded have a BICc-LER<0.5 indicating competing models.

w_i probability of ADAPT(1,0) (ADAPT(1,0) w_i=0.15) is more than half that of the optimum order (ADAPT(1,1) w_i=0.37). The BICc selected ADAPT(1,0) as the optimum order (wi=0.46), however, the BICc-LER for ADAPT(1,1) was low, 0.21 and wi= 0.28.

B. Tri-exponential Partial Volume Effect Models

1) Selection of Optimum Order

Mono-, bi- and tri- exponential fitting methods were applied to the PVE models (SNR ≈ 50) with varying CSF:WM ratios and the optimum fit selected using the AICc (Table III) and the BICc (Table IV). Based on the AICc, the number of detected components did not correspond to the number of exponential terms presented in the signal. In particular, a tri-exponential fit was found to best represent both two and three component models. The one compartment model was best represented by a bi-exponential fit. However, the LER-AICc values indicated that all other multi-exponential fits were competing. Based on the BICc, the one compartment and three compartment models were correctly identified but a two compartment model was overfitted and found to be best represented by a tri-exponential fit. No other multi-exponential fits were found to compete. According to the AICc and BICc, the two compartment model is wrongly fitted by a tri-exponential fit for even very high SNR≈100 (Figure 3).

The range of ADAPT orders from (0,0) to (3,3) were also applied to the PVE models (Table III). With the AICc, a distinct number of terms were found to be able to distinguish between two and three compartment models. The two and three compartment models were found to be best fitted by ADAPT orders (1,1) and (3,1) with no other competing order found to be significant. All other AICc-LERs were found to be >0.5, indicating that no other fit was significant. The BICc

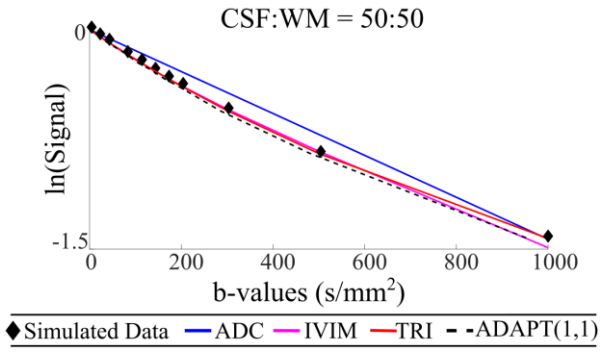

Fig.2. The optimum ADAPT order and the multi-exponential models are shown fitted to the PVE model CSF:WM 50:50. The ADAPT model demonstrates its ability to accurately fit and identify the tri-exponential signal.

results were found to be similar (Table IV), although ADAPT(1,1) was found to be a competing order (BICc-LER= 0.28) for the three compartment CSF:WM=25:75 signal. The one compartment CSF model was best fitted by ADAPT(1,1) according to the AICc and ADAPT(1,0) with the BICc. Both list a range of different orders as the optimum fit, indicating that noise can easily corrupt a one compartment signal. The one compartment signal was investigated at SNR≈100 and decisively found to be represented by ADAPT(0,0) (Fig. 4), mathematically equivalent to the mono-exponential equation.

Comparing the AICc values of the exponential and ADAPT fitting methods, for the one component signal, the AICc was lowest with ADAPT, indicating a better fit. However, the optimum AICc values are very similar and the RSS values are of the same order of magnitude (RSS for ADC = 1.2×10^{-5}, ADAPT(0,0) = 1.5×10^{-5}, ADAPT(1,1) = 4.0×10^{-6}). For the three component signals, the tri-exponential fits have much lower AICc values than ADAPT(3,1). The RSS values are also two orders of magnitude smaller (i.e RSS for CSF:WM-50:50, TRI = 4.3×10^{-5}, ADAPT(3,1) = 1.0×10^{-4}). For the two-component data, the wrongly identified tri-exponential fit has a very low RSS value (RSS for TRI = 4.5×10^{-6}, suggesting that the signal is being over fitted. Although the AICc for IVIM is still lower than ADAPT(1,1) (RSS for IVIM = 1.8×10^{-5}, ADAPT(1,1) = 7.2×10^{-5}), the RSS values are of the same order of magnitude, indicating a similar accuracy of fit.

2) Number of ADAPT Components

The transfer function, Z-transform, PFD and subsequent inverse Z-transform were performed on ADAPT(3,1) which was evaluated to be a three component decay model (Appendix B).

C. SNR and Robustness of Data Simulations

1) Influence of Noise upon the Tri-exponential Partial Volume Effects Model

Using the AICc-LERs, the ability for the multi-exponential fitting methods (Fig.3) and the ADAPT methods (Fig.4) to detect the number of components was investigated as a function of varying SNR. In the interest of concision, the BICc-LER was not considered. The multi-exponential fitting methods correctly identified the mono-exponential behavior in the PVE signal CSF:WM 100:0. However, the LER demonstrates that the optimum fit quickly becomes bi-exponential below the high SNR of 85. The three compartment PVE signals are best represented by the tri-

This article has been accepted for publication in a future issue of this journal, but has not been fully edited. Content may change prior to final publication. Citation information: DOI 10.1109/TBME.2019.2893523, IEEE Transactions on Biomedical Engineering

TABLE III
PARTIAL VOLUME EFFECT MODELS FITTED WITH ADAPT ORDERS AND MULTI-EXPONENTIAL FITTING METHODS-AICC

			Exponential Model			ADAPT Orders					
CSF:WM	Number of compartments		ADC	IVIM	TRI	(0,0)	(1,0)	(1,1)	(2,0)	(3,0)	(3,1)
100:0	1	AICc	-154	**-155**	-154	-154	-160	**-161**	-159	-161	-158
		LER_{AIC_c}	0.32	**0**	0.33	1.45	0.17	**0**	0.32	0.02	0.55
75:25	3	AICc	-67	-110	**-154**	-59	-79	-97	-78	-77	**-108**
		LER_{AIC_c}	18.85	9.40	**0**	10.65	6.13	2.32	6.48	6.75	**0**
50:50	3	AICc	-64	-108	**-152**	-60	-83	-101	-82	-80	**-110**
		LER_{AIC_c}	18.97	9.42	**0**	11.01	5.83	2.02	6.08	6.59	**0**
25:75	3	AICc	-68	-116	**-150**	-67	-92	-111	-91	-88	**-116**
		LER_{AIC_c}	17.77	7.47	**0**	10.75	5.29	1.13	5.40	6.08	**0**
0:100	2	AICc	-80	-140	**-151**	-81	-103	**-128**	-104	-102	-123
		LER_{AIC_c}	15.50	2.44	**0**	10.30	5.35	**0**	5.17	5.71	1.09

A range of PVE models, with varying CSF:WM ratios, were investigated. Multi-exponential fitting methods and the ADAPT method were fitted. The optimum fit was selected by choosing the method with the lowest AICc.

TABLE IV
PARTIAL VOLUME EFFECT MODELS FITTED WITH ADAPT ORDERS AND MULTI-EXPONENTIAL FITTING METHODS-BICC

		Exponential Model			ADAPT Orders					
CSF:WM		ADC	IVIM	TRI	(0,0)	(1,0)	(1,1)	(2,0)	(3,0)	(3,1)
100:0	BICc	**-149**	-144	-139	**-152**	**-155**	-150	-151	-153	-144
	LER_{BIC_c}	**0**	0.94	2.02	**0.72**	**0**	1.09	0.75	0.45	2.40
75:25	BICc	-62	-100	**-139**	-56	-74	-89	-70	-66	**-93**
	LER_{BIC_c}	16.84	8.64	**0**	8.07	4.12	0.91	5.07	6.00	**0**
50:50	BICc	-59	-97	**-137**	-57	-78	-93	-74	-69	**-96**
	LER_{BIC_c}	16.95	8.66	**0**	8.43	3.81	0.61	4.66	5.84	**0**
25:75	BICc	-63	-105	**-136**	-64	-87	**-103**	-83	-77	**-102**
	LER_{BIC_c}	15.75	6.72	**0**	8.44	3.55	**0**	4.27	5.61	**0.28**
0:100	BICc	-75	-129	**-137**	-78	-98	**-120**	-96	-91	-109
	LER_{BIC_c}	13.48	1.69	**0**	9.13	4.75	**0**	5.17	6.37	2.50

The optimum fitting method for the PVE models (SNR≈ 50) was also selected by choosing the method with the lowest BICc.

exponential fit down to a SNR of 35 for the CSF:WM of 75:25 and 50:50, and SNR 40 for 25:75. The PVE signal CSF:WM 0:100 is incorrectly represented by a tri-exponential fit. This however becomes a bi-exponential fit below below SNR 50. CSF:WM 100:0 is best represented by the one component ADAPT(0,0) above a SNR of 75. Below SNR 75 the one component ADAPT(1,0), is the optimum order. However, ADAPT(2,0) and ADAPT(3,0) have AICc-LERs<0.5, indicating significant competing fitting methods. All three compartment PVE models are best represented by the three component ADAPT(3,1) down to an SNR of 45. For CSF:WM 0:100, the optimum order is the two component model ADAPT(1,1) down to a SNR of 45. Below this value the one component models and ADAPT (2,0), another two component model, begin to show significance.

D. ADAPT Components Applied to In Vivo Data Acquisition

The ADAPT method was applied to a DWI axial slice of both a volunteer and a patient case (Fig. 5). Three ADAPT components are observed as a white line along the boundary of the ventricles for the volunteer case (Fig. 5c). Such clusters of high order behavior could be caused by partial volume effects. Few voxels exhibit one-component behavior in the ventricles of the volunteer. This could be due to the limited size of the ventricles. A patient case was considered in which the ventricles were enlarged. Large clusters of one component behavior were observed (Fig.5d).

E. ADAPT(1,1) Coefficient Study with Data Simulations

The relationship between the ADAPT α and β coefficients, created as a result of minimizing (2), and the IVIM f, D and D* parameters were investigated (Fig. 6). If IVIM-f and IVIM-D* are fixed and only IVIM-D is varied for simulated data, the gradient of the detected diffusion signal can be observed to increase with an increasing IVIM-D value (Fig. 6a). An increase in the gradient of the signal would also increase the value of the ADAPT-β coefficients and result in a directly linear relationship between the IVIM-D and ADAPT(1,1)-β_0 with R^2=1(Fig. 6d). When IVIM-f and IVIM-D are fixed, increases in IVIM-D* result in a subtle increase in the gradient at the low b-values (Fig. 6c). Such behaviour results in a linear correlation between IVIM-D* and the higher order ADAPT(1,1)- β_1 coefficient with R^2=0.99 (Fig. 6f). When IVIM-D and IVIM-D* are fixed and only IVIM-f is varied, an increase in IVIM-f results in an increase in the curvature of the bi-exponential signal and the prevalence of the second component (Fig. 6b). Consequently a linear relationship is found between IVIM-f and ADAPT(1,1)-α_1 with R^2=0.99 (Fig. 6e).

The coefficients of ADAPT and the multi-exponential fitting methods were investigated for the PVE models (SNR≈50) (Fig. 7). For the one compartment model, the optimum mono-exponential fitting method and ADAPT(1,0) were considered. ADAPT(0,0) was also considered due to

This article has been accepted for publication in a future issue of this journal, but has not been fully edited. Content may change prior to final publication. Citation information: DOI 10.1109/TBME.2019.2893523, IEEE Transactions on Biomedical Engineering

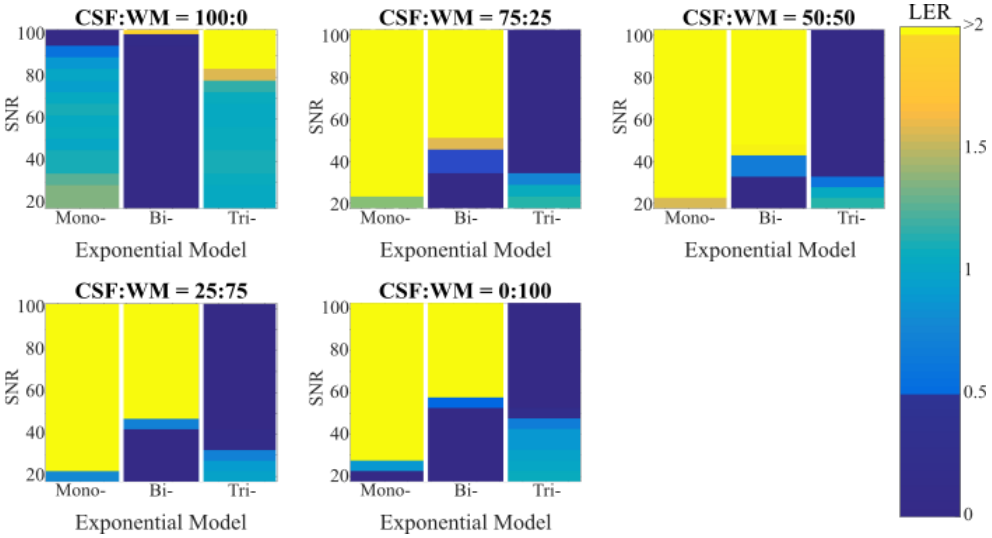

Fig.3. Using the AICc-LERs, the ability for the multi-exponential fitting methods to detect the number of components in the PVE models was investigated as a function of varying SNR. An AICc-LER<0.5 indicates a competing model that needs to be considered. An AICc-LER>2 indicates a competing model that 'definitely' does not need to be considered.

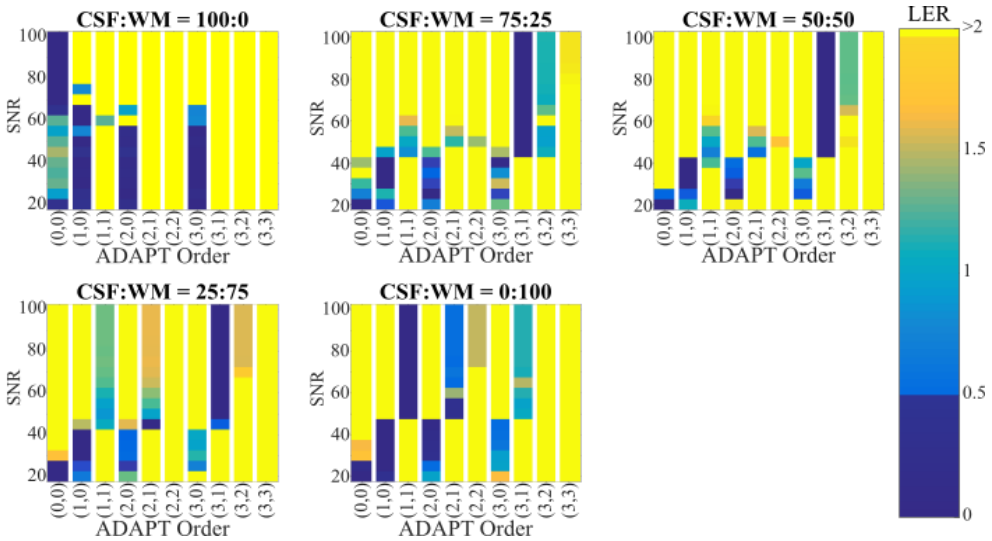

Fig.4. Using the AICc-LERs, the ability for the ADAPT method to detect the number of components in the partial volume effect models was investigated as a function of varying SNR.

being mathematically equivalent to the mono-exponential equation. The CV was found to be 0.4% for the mono-exponential ADC and 0.2% for ADAPT(0,0)-β_0. Both have a CV <1% indicating that both fitting methods are robust for fitting one compartment data. For ADAPT(1,0), β_0 had a CV of 0.6% and α_1 2735.7%. The β_0 coefficients from ADAPT(0,0) and ADAPT(1,0) had a percentage variation of 0.0002%. Given the similarity in β_0 coefficients and the high CV for ADAPT(1,0)-α_1, it can be theorized that the additional parameter in the one component ADAPT(1,0) is a consequence of the noise added to the signal. For the three compartment models, the optimum fitting methods, ADAPT(3,1) and the tri-exponential fit were compared. In general, the ADAPT(3,1) coefficients have a lower CV than the tri-exponential parameters. α_2 and α_3 have a higher CV than the TRI-f_{CSF} and f_{WM} parameters for the CSF:WM=50:50 case, but the CV is still less than 6.1%. For the CSF:WM=25:75 case, the TRI-f_{CSF} has a CV of 13.2% significantly higher than any of the other parameters associated with three compartments. For the two compartment model, ADAPT(1,1) was compared against both the bi- and tri- exponential fitting methods. Although selected as the optimum multi-exponential fit, it is evident that the tri-exponential is the incorrect fit as the CV of TRI-f_{CSF} is 193.0%. Comparing the ADAPT(1,1) coefficients to the IVIM parameters, β_0, β_1, and α_1 had CVs of 0.4%, 2.8% and 0.8% respectively. IVIM-D, IVIM-D* and IVIM-F were 0.3%, 2.2% and 2.9%. Both methods possessed low CVs for their parameters indicating that ADAPT(1,1) and IVIM are both robust fitting methods for two compartment signals.

F. ADAPT(1,1) Coefficient Study with In Vivo Data

The ADAPT(1,1)-β_0 (Fig. 8b), α1 (Fig. 8d) and β_1 (Fig. 8f) coefficients for an in vivo axial slice of a patient brain scan were correlated on a pixel-wise basis with the IVIM-D (Fig. 8a), IVIM-f (Fig. 8c) and IVIM-D* (Fig. 8e) parameters respectively. Upon visual inspection, the IVIM-D and ADAPT(1,1)-β_0 parametric maps appear similar with the calibration bars also showing comparable scales. Furthermore, when the voxels with ADAPT(1,1) as their optimum order were selected (n=6002), ρ=0.708 (P <0.001) was obtained, indicating a strong relationship between IVIM-D and

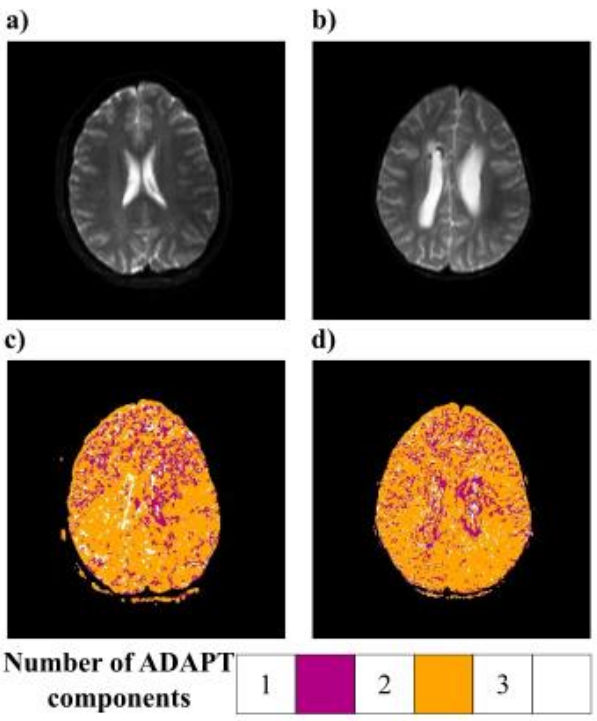

Fig.5. Example case of the ADAPT method applied to in vivo DWI axial slices. a) DWI slice of volunteer where b value=0 s/mm^2. b) DWI slice of patient with enlarged ventricles where b value=0 s/mm^2 c) ADAPT applied to volunteer slice and the corresponding number of detected components are displayed. f) ADAPT applied to patient slice.

ADAPT(1,1)-β_0. However, the edges of the ventricles appear to be affected by partial volume effects more in the IVIM maps than the ADAPT maps. IVIM-D* and ADAPT(1,1)-β_1 were found to have a $\rho = 0.741$ (P<0.001), also indicating a strong relationship. The CPU run time of the IVIM fit for one slice was averaged over 10 iterations and found to be 575.0 ± 3.1 seconds. Comparatively the CPU run time of ADAPT method was just 23.2 ± 0.1 seconds.

The CV was calculated from the average coefficient values calculated from ROIs within the CSF and WM (Table V). For the one compartment CSF, ADAPT(0,0)-β_0 was almost identical to the ADC value and the CV >1.5%. For the two compartment WM, ADAPT(1,1)-β_0 was found to be the same order of magnitude as IVIM-D although the CV of IVIM-D was found to be just 4.6% compared to 10.7% for β_0. However, ADAPT(1,1)-α_1 has a lower CV than IVIM-f 16.7% compared to 18.2%. ADAPT(1,1)-β_1 has a significantly lower CV than IVIM-D*, 25.0% compared to 78.7%.

IV. Discussion

It has been demonstrated that the number of components in diffusion-weighted MRI data is determined unreliably by simply applying multi-exponential fitting methods and then selecting the optimum fit. The ADAPT method is superior at identifying multiple components, even when the third component is more subtle, i.e. PVE model with CSF:WM 75:25. However, the BICc did detect competing orders, indicating that the third compartment could be difficult to detect for cases where the fraction of CSF is even more subtle. Although the tri-exponential fitting methods had lower RSSs than ADAPT(3,1) for the three compartment PVE models, the

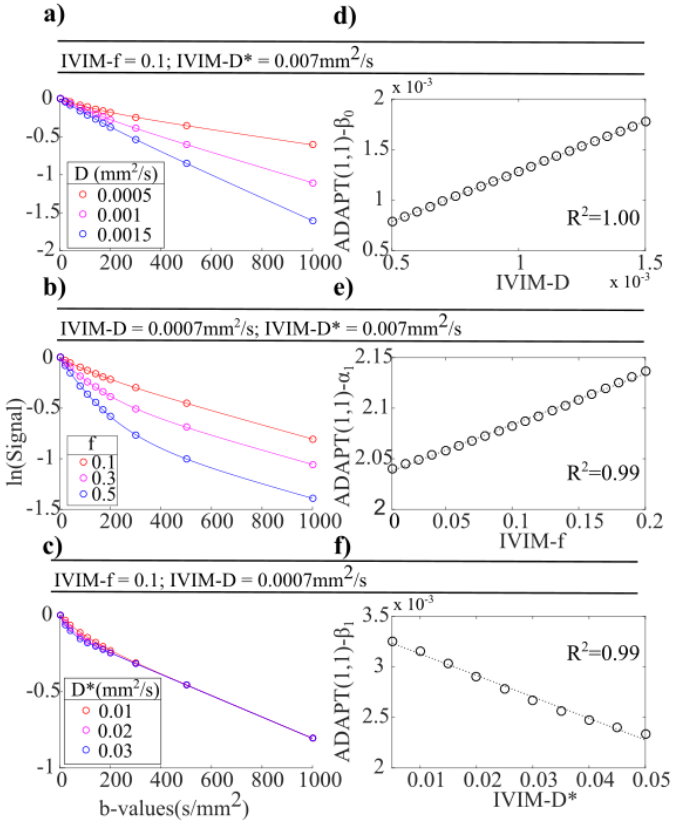

Fig.6. The relationship between the ADAPT(1,1) coefficients and the IVIM parameters was investigated. a) Effects on the diffusion signal when only IVIM-D is varied and the other two IVIM parameters are fixed. b) Only IVIM-f varied. c) Only IVIM-D* varied. d) Linear relationship between IVIM-D and ADAPT(1,1)-β_0. e) Between IVIM-f and ADAPT(1,1)-α_1. f) Between IVIM-D* and ADAPT(1,1)-β_1.

low RSSs is more likely due to the study being culpable of the inverse crime (see below) and the tri-exponential fitting method being inherently biased towards the simulated tri-exponential data. Furthermore, the RSS values for the optimum ADAPT orders are still low and the model selection is more robust. It is recommended that if the number of compartments in a signal is unknown, the ADAPT method should be used instead of multi-exponential fitting for model selection. The ADAPT method also demonstrated that it could correctly identify the number of components in the bi-exponential signal across a large range of IVIM parameter values. The SNR analysis demonstrated that ADAPT was more robust at detecting both one and two compartment signals. ADAPT is a generalization of exponential models and makes no prior assumptions about the number of components within the data. Thus ADAPT lends itself as a potential novel method for the detection of the number of components in DWI data and potentially for providing more intricate diffusion biomarkers. The data simulations indicated that there is a relationship between the IVIM parameters and ADAPT coefficients. A strong relationship between these two methods is also evident in the in vivo patient example. Although the relationship between the IVIM parameters and ADAPT coefficients is complex and non-linear in nature, ADAPT presents the opportunity for complex diffusion biomarkers to be obtained by making no prior assumptions about the nature

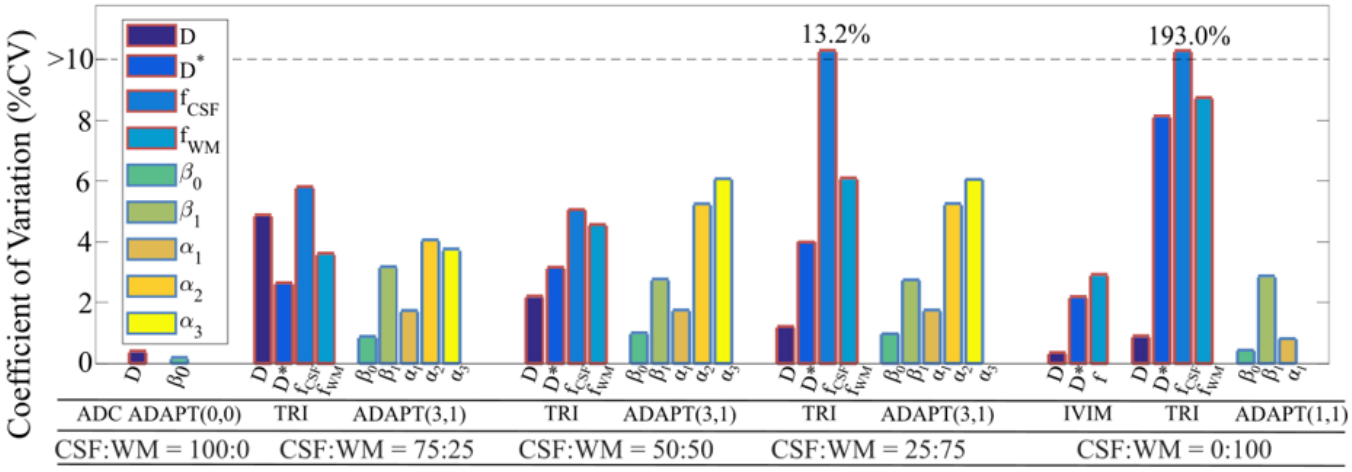

Fig.7. Coefficient of Variation calculated for the optimum ADAPT and multi-exponential fitting methods for each of the PVE models (SNR ≈ 50) considered.

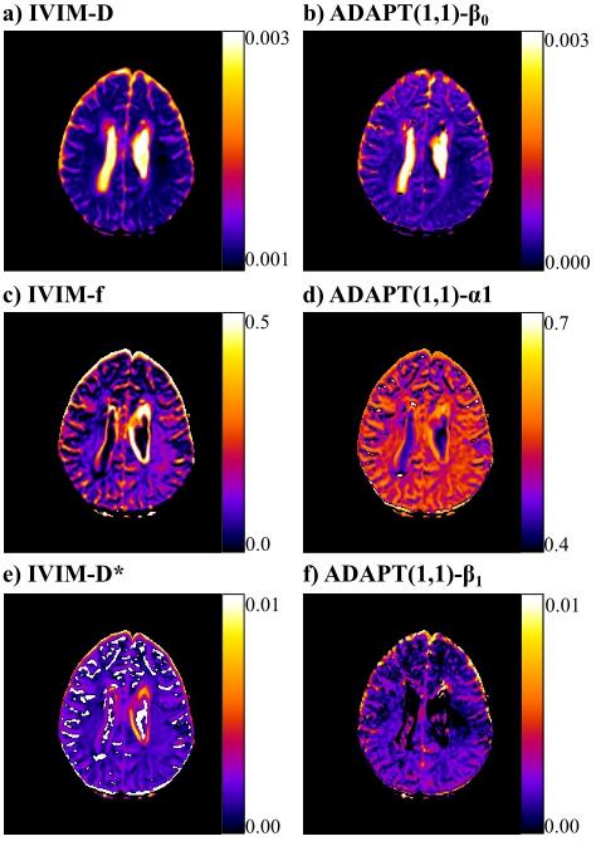

Fig.8. Parametric maps of Axial brain slice of patient with enlarged ventricles a) IVIM-D (mm^2/s); c)IVIM-f; e)IVIM-D* (mm^2/s); b) ADAPT(1,1)-β_0; d)ADAPT(1,1)-α_1; f)ADAPT(1,1)-β_1.

of the data nor does it require any multistep fitting processes. Consequently, in this study, ADAPT is a much faster fitting method. The in vivo ROIs showed that ADAPT(1,1) and IVIM had comparable parameter CVs. However, IVIM-D* was considerably higher. Although this may be due to tissue heterogeneity within the white matter, the average IVIM-D* value is higher than expected, indicating that ADAPT may be more robust than IVIM at fitting WM.

Both the ADAPT and multi-exponential fitting methods struggled to correctly identify the number of signal components at poor SNRs (< 45). The addition of noise to the tri-exponential PVE models resulted in the methods under-

TABLE V
OPTIMUM FITTING METHODS APPLIED TO IN VIVO ROIS- PARAMETER COEFFICIENT OF VARIATION (CV)

Number of compartments	Parameter	Average	Standard Deviation.	CV (%)
1	ADC	2.89E-03	4.04E-05	1.40
	(0,0)-b0	2.90E-03	3.73E-05	1.30
2	IVIM-D	8.66E-04	4.01E-05	4.64
	(1,1)-b0	6.24E-04	6.71E-05	10.77
	IVIM-D*	4.66E-02	3.67E-02	78.65
	(1,1)-b1	1.01E-03	2.53E-04	24.98
	IVIM-f	0.074	0.013	18.16
	(1,1)-a1	0.601	0.100	16.65

ROIs were drawn within the WM and CSF on the patient axial slice (Fig. 5b). The parameter values for the optimum methods were calculated.

fitting the signal. This was most likely due to noise modulating the true signal and causing individual components to be mistakenly classified together. The addition of noise to the mono-exponential fitting method resulted in the over fitting the signal. Although ADAPT was still able to detect a one component model at poor SNR, the optimum order, using the AICc, switched from ADAPT(0,0) to ADAPT(1,0) resulting in an additional parameter. Although more robust than the multi-exponential fitting methods, the ADAPT method requires further development to optimize how it handles low SNR data and the inclusion of an additional component or parameter to account for noise should be considered.

In general the AICc and BICc selected the same optimum order, increasing the confidence that the most appropriate order had been selected. However, a more formal protocol is required for when the information criterions disagree.

One should note that only one range of clinically relevant b-values was considered for the data simulated or acquired in vivo in this study. The number of data points and their magnitude could have a significant influence on the performance of the ADAPT method and the generality of the findings. However, there is no clear consensus on what optimal b-value sequence should be used for DWI [30]. As the

ADAPT method requires a discrete approximation of the diffusion signal, there will inevitably be a truncation in the approximation which is inherent to the method. Another limitation of the simulations in this study was the assumption that diffusion in the CSF exhibits mono-exponential behavior, consequently the effects of CSF circulation or pulsatile flow [31] were not considered. However, the method presented remains a useful test for detecting multiple components.

As far as the authors are aware, no other diffusion models with a perfusion fraction exist for simulating data other than the multi-exponential equations explored. Hence it was not possible to avoid committing the 'inverse crime' (IC) where multi-exponential equations were used to simulate as well as fit the data. In order to mitigate the IC, Gaussian noise was added to the simulated data [32] and a range of different multi-exponential models were explored. In addition, the ADAPT method is a different mathematical model and therefore the IC wasn't committed with this class of models.

The study only considered DWI data, which averages over all the directions in which a gradient is applied. Consequently this method is only able to measure isotropic diffusion compartments. If anisotropic effects, such as fanning or crossing of axon bundles, were to be investigated, many diffusion weighted images, with diffusion weighted gradients in different directions, would be required resulting in Diffusion Tensor Imaging (DTI). Although multi b-value models are not yet routine in clinical settings[4], it would be interesting to consider an application of ADAPT to this technique, in particular investigating anisotropic effects with further simulations and in vivo studies.

Further investigations are required to understand how the number of optimum ADAPT components relates to the number of exponential terms within the signal. The transfer function requires further rearrangement to enable the inverse Z-transform solution to be in the form of a summation of multi-exponential compartments.

V. Conclusion

The ADAPT method has shown that it can distinguish between multi-exponential diffusion data containing different numbers of components. This is something that cannot be achieved by applying multi-exponential fitting methods and selecting the optimum fit. Such a novel method allows for the identification of different components within a diffusion signal. The relationship between the ADAPT and IVIM parameters suggest that potential complex diffusion biomarkers can be obtained by making no prior assumptions about the nature of the data. Whilst ADAPT has been applied to DWI data, it should find application in other discrete data sets which can be manipulated to be represented as a function of acquisition points.

Appendix

A. Bayes Factor-Associated Statistics

The Akaike weight, w_i indicates the probability of model i being the optimum model:

$$w_i = \frac{\exp(-\frac{1}{2}\Delta_i AICc)}{\sum_{m=1}^{M}\exp(-\frac{1}{2}\Delta_m AICc)} \quad (12)$$

Where M is the number of compared models and:

$$\Delta_i AICc = AICc(i) - AICc_{min} \quad (13)$$

Where $AICc_{min}$ is the minimum AICc value of all the models considered. The Akaike weight of all the models summed together should equal one. The Evidence Ratio ER:

$$ER_i = \frac{w_{max}}{w_i} \quad (14)$$

Where w_{max} is the Akaike weight of the optimum model. The LER is provided by taking the log of the ER such that.

$$LER_i = \log_{10}(ER_i) \quad (15)$$

B. Derivation of the Number of ADAPT Components

ADAPT(1,0) gives:

$$\ln(S_n) = \beta_0 b_n + \alpha_1 \ln(S_{n-1}) \quad (16)$$

And the transfer function of ADAPT(1,0) in the Z-domain:

$$H(z) = \frac{\beta_0 z}{z-\alpha_1} \quad (17)$$

Performing partial fraction decomposition (PFD) and an Inverse Z transform:

$$H(n) = \beta_0 {\alpha_1}^n \quad (18)$$

Hence ADAPT(1,0) was also evaluated to be a one component decay model. ADAPT(2,0) gives:

$$\ln(S_n) = \beta_0 b_n + \alpha_1 \ln(S_{n-1}) + \alpha_2 \ln(S_{n-2}) \quad (19)$$

And the transfer function of ADAPT(2,0) in the Z-domain:

$$H(z) = \frac{\beta_0 z^2}{z^2-\alpha_1-\alpha_2} = \frac{\beta_0 z^2}{(z-r_1)(z-r_2)} \quad (20)$$

Where the denominator is factorized such that r_1 and r_2 are roots of the quadratic expression. Performing PFD and an Inverse Z transform:

$$H(n) = A{r_1}^{n-1} + B{r_2}^{n-1} \quad (21)$$

Where A and B represent the numerators that would be attained through the PFD. Hence ADAPT(2,0) was also evaluated to be a two component decay model. ADAPT(2,1) gives:

$$\ln(S_n) = \beta_0 b_n + \beta_1 b_{n-1} + \alpha_1 \ln(S_{n-1}) + \alpha_2 \ln(S_{n-2}) \quad (22)$$

And the transfer function of ADAPT(2,1) in the Z-domain:

$$H(z) = \frac{\beta_0 z^2 + \beta_1 z}{z^2 - \alpha_1 - \alpha_2} \quad (23)$$

Performing PFD and an Inverse Z transform:

$$H(n) = C{r_1}^{n-1} + D{r_2}^{n-1} \quad (24)$$

`Where r_1 and r_2 are roots of the quadratic expression in the denominator of the transfer function and C and D represent the numerators that would be attained through the PFD. Hence ADAPT(2,1) was also evaluated to be a two component decay model. ADAPT(3,1) gives:

$$\ln(S_n) = \beta_0 b_n + \beta_1 b_{n-1} + \alpha_1 \ln(S_{n-1}) + \alpha_2 \ln(S_{n-2}) + \alpha_3 \ln(S_{n-3}) \quad (25)$$

And the transfer function of ADAPT(3,1) in the Z-domain:

$$H(z) = \frac{\beta_0 z^2 + \beta_1 z}{z^3 - \alpha_1 z^2 - \alpha_2 z - \alpha_3} = \frac{\beta_0 z^2 + \beta_1 z}{(z - r_1)(z - r_2)(z - r_3)} \quad (26)$$

Where the denominator is factorized such that r_1, r_2 and r_3 are roots of the cubic expression. Performing PFD and an Inverse Z transform:

$$H(n) = F{r_1}^{n-1} + G{r_2}^{n-1} + H{r_3}^{n-1} \quad (27)$$

Where F, G and H represent the numerators that would be attained through the PFD. Hence ADAPT(3,1) was evaluated to be a three component decay model.

REFERENCES

[1] Y. Ueda, S. Takahashi, N. Ohno, K. Kyotani, H. Kawamitu, T. Miyati, *et al.*, "Triexponential function analysis of diffusion-weighted MRI for diagnosing prostate cancer," *J Magn Reson Imaging*, vol. 43, pp. 138-48, Jan 2016.

[2] N. Ohno, T. Miyati, S. Kobayashi, and T. Gabata, "Modified triexponential analysis of intravoxel incoherent motion for brain perfusion and diffusion," *J Magn Reson Imaging*, vol. 43, pp. 818-23, Apr 2016.

[3] G. Fournet, J. R. Li, A. M. Cerjanic, B. P. Sutton, L. Ciobanu, and D. Le Bihan, "A two-pool model to describe the IVIM cerebral perfusion," *Journal of Cerebral Blood Flow and Metabolism*, vol. 37, pp. 2987-3000, Aug 2017.

[4] G. S. Chilla, C. H. Tan, C. Xu, C. L. Poh, "Diffusion weighted magnetic resonance imaging and its recent trend-a survey," *Quantitative Imaging in Medicince and Surgery*, vol. 5, pp. 407-422, Jun 2015.

[5] J. E. Tanner, "Pulsed Field Gradients for Nmr Spin-Echo Diffusion Measurements," *Review of Scientific Instruments*, vol. 36, pp. 1086-&, 1965.

[6] D. Le Bihan and E. Breton, "Imagerie de diffusion in-vivo par résonance magnétique nucléaire," *Comptes-Rendus de l'Académie des Sciences*, vol. 93, pp. 27-34, 1985-12 1985.

[7] D. Le Bihan, E. Breton, D. Lallemand, P. Grenier, E. Cabanis, and M. Laval-Jeantet, "MR imaging of intravoxel incoherent motions: application to diffusion and perfusion in neurologic disorders," *Radiology*, vol. 161, pp. 401-7, Nov 1986.

[8] E. M. Meeus, J. Novak, H. Dehghani, and A. C. Peet, "Rapid measurement of intravoxel incoherent motion (IVIM) derived perfusion fraction for clinical magnetic resonance imaging," *MAGMA*, Oct 26 2017.

[9] M. Kim and H. S. Kim, "Emerging Techniques in Brain Tumor Imaging: What Radiologists Need to Know," *Korean Journal of Radiology*, vol. 17, pp. 598-619, Sep-Oct 2016.

[10] D. G. Gardner, J. C. Gardner, G. Laush, and W. W. Meinke, "Method for the Analysis of Multicomponent Exponential Decay Curves," *Journal of Chemical Physics*, vol. 31, pp. 978-986, 1959.

[11] E. M. Landaw and J. J. Distefano, "Multiexponential, Multicompartmental, and Noncompartmental Modeling .2. Data-Analysis and Statistical Considerations," *American Journal of Physiology*, vol. 246, pp. R665-R677, 1984.

[12] J. Ponce Hornos and M. F. Villamil, "A simple method for fitting multi-exponential curves of the decay type in a hand calculator," *Acta Physiol Lat Am*, vol. 30, pp. 141-6, 1980.

[13] J. F. Hauer, C. J. Demeure, and L. L. Scharf, "Initial Results in Prony Analysis of Power-System Response Signals," *Ieee Transactions on Power Systems*, vol. 5, pp. 80-89, Feb 1990.

[14] A. U. J. M.-J. E. Salami, "An Appraisal of Gardner Transform-Based Methods of Transient Multiexponential Signal Analysis," *International Journal of Computer Theory and Engineering*, vol. 4, pp. 16-25, February 2012.

[15] P. Whittle, *Hypothesis testing in time series analysis*. Uppsala,: Almqvist & Wiksells boktr., 1951.

[16] G. E. P. J. Box, Gwilym M.; Reinsel, Gregory C.; Ljung, Greta M, *Time Series Analysis: Forecasting and Control (5th ed.)*. . New Jersey: Wiley, 2016.

[17] A. Lemke, B. Stieltjes, L. R. Schad, and F. B. Laun, "Toward an optimal distribution of b values for intravoxel incoherent motion imaging," *Magn Reson Imaging*, vol. 29, pp. 766-76, Jul 2011.

[18] C. Federau, "Intravoxel incoherent motion MRI as a means to measure in vivo perfusion: A review of the evidence," *NMR Biomed*, vol. 30, Nov 2017.

[19] D. Le Bihan and M. Iima, "Diffusion Magnetic Resonance Imaging: What Water Tells Us about Biological Tissues," *PLoS Biol*, vol. 13, p. e1002203, Jul 2015.

[20] W. C. Wu, Y. F. Chen, H. M. Tseng, S. C. Yang, and P. C. My, "Caveat of measuring perfusion indexes using intravoxel incoherent motion magnetic resonance imaging in the human brain," *European Radiology*, vol. 25, pp. 2485-2492, Aug 2015.

[21] E. M. Meeus, J. Novak, S. B. Withey, N. Zarinabad, H. Dehghani, and A. C. Peet, "Evaluation of intravoxel incoherent motion fitting methods in low-perfused tissue," *J Magn Reson Imaging*, Aug 22 2016.

[22] NEMA, "Determination of signal-to-noise ratio (SNR) in diagnostic magnetic resonance imaging," *NEMA*, 2001.

[23] H. Akaike, "A New Look at the Statistical Model Identification " *IEEE Transactions on Automatic Control*, vol. 19, pp. 716-723, 1974.

[24] J. E. Cavanaugh, "Unifying the derivations for the Akaike and corrected Akaike information criteria," *Statistics & Probability Letters*, vol. 33, pp. 201-208, Apr 30 1997.

[25] E. Panagiotaki, T. Schneider, B. Siow, M. G. Hall, M. F. Lythgoe, and D. C. Alexander, "Compartment models of the diffusion MR signal in brain white matter: A taxonomy and comparison," *Neuroimage*, vol. 59, pp. 2241-2254, Feb 1 2012.

[26] G. Schwarz, "Estimating the dimensions of a model",*The Annals of Statistics*, vol. 6, pp. 461-464 Mar 1978.

[27] A. D. McQuarrie, "A small-sample correction for the Schwarz SIC model selection criterion," *Statistcs and Probability Letters*, vol. 44, pp. 79-86, Aug 1999.

[28] H. Akaike, "Prediction and Entropy", in Selevted Papers of Hirotugu Akaike, Springer, New York, pp. 387-410, 1985.

[29] R. E. Kass and A. E. Raftery, "Bayes Factors," *Journal of the American Statistical Association*, vol. 90, pp. 773-795, Jun 1995.

[30] B. Taouli, A. J. Beer, T. Chenevert, D. Collins, C. Lehman, C. Matos, *et al.*, "Diffusion-weighted imaging outside the brain: Consensus statement from an ISMRM-sponsored workshop," *Journal of Magnetic Resonance Imaging*, vol. 44, pp. 521-540, Sep 2016.

[31] L. E. Salminen, T. E. Conturo, J. D. Bolzenius, R. P. Cabeen, E. Akbudak, and R. H. Paul, "Reducing Csf Partial Volume Effects to Enhance Diffusion Tensor Imaging Metrics of Brain Microstructure," *Technol Innov*, vol. 18, pp. 5-20, Apr 2016.

[32] C.E. Chavez, F. Alonzo-Atienza, D. Alvarez, "Avoiding the Inverse Crime in the Inverse Problem of Electrocardiography: Estimating the Shape and Location of Cardiac Ischemia, *Computing in Cardiology*, vol. 40, pp. 697-690, Sep 2013.